Heliyon 10 (2024) e26148

Contents lists available at ScienceDirect

Heliyon

journal homepage: www.cell.com/heliyon

Research article

Estimating natural frequency of pipe with various geometries: Improvement of frequency factors

Noor Fariza Saari [a], Azma Putra [a,*], Irianto [b], Reduan Mat Dan [a], Muhammad Agus Zeli [a], Roszaidi Ramlan [a], Nawal Aswan Abdul Jalil [c], Safarudin Herawan [d]

[a] *Fakulti Teknologi dan Kejuruteraan Mekanikal, Universiti Teknikal Malaysia Melaka, Hang Tuah Jaya, 76100, Durian Tunggal, Malaysia*
[b] *Faculty of Resilience, Rabdan Academy, Abu Dhabi P.O. Box 114646, United Arab Emirates*
[c] *Department of Mechanical and Manufacturing Engineering, Faculty of Engineering, Universiti Putra Malaysia, 43400, Serdang, Malaysia*
[d] *Department of Industrial Engineering, Bina Nusantara University, Jakarta, 11480, Indonesia*

ARTICLE INFO

Keywords:
Natural frequency
Piping vibration
Resonance
Pipe bend
Fluid-induced vibration

ABSTRACT

Piping system is the main structure in many industrial applications, especially for large industry relating with processing and transporting fluids, such as oil and gas industries. The fluid-induced vibration is often the cause of structural fatigue in pipes and therefore piping vibration need to be closely monitored. In case of high piping vibration, knowledge of the natural frequency of a pipe section is crucial for an engineer to propose the right troubleshoot action, either for a temporary or even for a long-term solution for the piping vibration. Therefore, prediction of the pipe natural frequency using a simple formulae is thus of interest, without dealing with complex numerical simulation using a commercial software which consumes cost and time. In this paper, the vibration mode shapes of various possible geometries of pipes in practice were simulated in ANSYS and the simulated natural frequency is related to a natural frequency of an Euler-Bernoulli beam using a correction factor for each corresponding piping geometry. This paper extends the previous work by allowing the boundary conditions of the pipe ends to be simply supported, in addition to the clamped edges. In this way, the frequency factor charts are presented in the range of possible correction factor values to accommodate the real conditions of pipe arrangement in practical application. An experiment from a case study to verify the proposed method is also presented.

1. Introduction

Piping system has a primary function in wide range of industries especially in oil and gas industry. The vibration level of the piping system must always be monitored to avoid structural piping failure such as fatigue and leaks, which can lead to process downtime and can even initiate a hazard condition. Excessive piping vibration can be generated by pulsation induced flow, turbulence induced flow, mechanical excitation from a rotating machine, water hammer, slug flow and also acoustics induced. Understanding the excitation frequency and determining the natural frequency of the pipe are crucial to perform a correct vibration control after the piping vibration assessment [1]. Many works have been published presenting method of predicting natural frequencies of a pipe.

Yi-min et al. [2] studied the natural frequency of a straight pipeline conveying fluid with simply-supported ends to indicate the effect of the flow velocity on the natural frequency by using the eliminated element-Galerkin method with different boundary for the

* Corresponding author.
E-mail address: azma.putra@utem.edu.my (A. Putra).

https://doi.org/10.1016/j.heliyon.2024.e26148
Received 24 May 2023; Received in revised form 7 February 2024; Accepted 8 February 2024
Available online 14 February 2024

natural frequency equations. Similarly, Liu and Wang [3] also utilized Galerkin's method for a dynamic model of a cantilevered horizontal piping system which conveying gas-liquid, two-phase slug flow to analyze its natural frequency. Yi-min et al. [4] later proposed a direct method to calculate the pipe natural frequency as an alternative to the method in Ref. [2]. Bao-hui et al. [5] modified the 4-equation model of a pipe conveying fluid proposed by Tijsseling et al. [6] by taking into account the dynamics of the inner fluid. By using the dynamic stiffness model, the natural frequencies of a simply supported pipe was determined. The calculation of the natural frequency was then extended into a case of a pipe with three spans (the pipe is also simply supported in the mid span). The accuracy was determined by comparing the values with those obtained from numerical simulation using ABAQUS software with the relative error of less than 1%. By employing the Differential Quadrature Method (DQM), Hu and Zu [7] calculated the first critical frequency of a curved-pipe, showing that a curved pipe can have significant different of critical frequency compared with that of the straight pipe.

Gu et al. [8] studied the aspect ratio of length to diameter (L/D) on the dynamic response of a fluid-conveying pipe using the Timoshenko beam model. It was found that the natural frequencies decrease with the increasing of internal fluid velocity and the critical velocity decreases with the decreasing of aspect ratio and the mode number. For high aspect ratio, where $L/D > 20$ for the first mode and $L/D > 40$ for the second mode, the Euler-Bernoulli model can be used as a good approximation. Koo and Park [9] studied the response of three-dimensional piping system conveying fluid for straight and curved pipe sections. The wave approach was used utilising the dynamic stiffness matrix and transfer matrix technique to calculate the frequency response. The results were then compared with those from the finite element method. Most recently, Zhang et al. [10] utilized experimental modal parameters (natural frequencies, damping ratios, and mode shapes) to determine the location of elastic supports in an L-shaped pipe to modify its natural frequencies for addressing the resonance problems.

The proposed analytical or semi-analytical models often model the pipe as a beam, by assuming the bending vibration of a hollow tube is similar to a beam (with rectangular cross section). Thus studies on the piping vibration using computational-aided simulation technique (Finite Element Model) have been widely used to effectively provide the numerical results and can be more convenient as it provides more flexibility to model the pipe as in the actual condition [11–14]. Apart from providing the natural frequencies and mode shapes of the pipe, FEM can also simulate the strain and stress across the length of the pipe. Performing simulation in FEM however, can be time consuming and costly. Accurate details of the pipe structure need to also be input for accurate results.

The natural frequency of pipe can also be determined by means of experiment. In practice, a bump test is a procedure commonly used by using a hammer to strike the pipe structure [15]. It must be noted that to obtain a good result of vibration response for the first and second modes, the piping structure must be sufficiently moved during the strike. Hence, this is often not possible in many case especially for a pipe with large diameter. Some of the pipe configurations in practice are also impossible to be tested due to the limit accessibility and hazard precaution.

Thus, a simple estimation of piping natural frequency is crucial for engineers to be able to provide a quick decision to the corresponding vibration problem for a troubleshoot, before a proper simulation study or vibration measurement is performed. Wachel et al. [16] proposed a simplified method to predict the natural frequency of pipes with various possible geometries of pipe spans with clamped edges. The relationship between piping vibration displacement, velocity and stress were also presented to indicate the piping severity.

Most piping systems in practice utilise clamping mechanism (also called 'pipe shoe') to support the piping structure. However depending on the type of clamping supports, not all the supports can be assumed to have a rigid clamp (constraint in displacement and rotation) as given in Ref. [16]. This paper extends the work in Ref. [16] by considering the pipe to have simply supported edges instead of clamped supports to allow a certain degree of structural motion at the location of the pipe support. The frequency factor charts are then calculated, presented with the range of values corresponding to simply supported and clamped edges for each pipe geometry, aiming at providing range of possibility of calculated natural frequency depending on the condition of the support.

2. Modelling piping natural frequencies

The pipe geometries can be divided into four general spans as shown in Fig. 1, representing the pipe sections mostly found in engineering practice [1]. For each span, the pipe is usually supported (either by rigid clamped, by spring support, etc) at both edges, which localise it from the other sections of connecting pipes and thus analysis of the piping vibration can be performed in this corresponding pipe span. The section length of the pipes: *A, B* and *C* are varied in the proposed formula to obtain a representative frequency factor for all possible length ratios.

2.1. General formulae

The natural frequency used is generalised for the natural frequency identical for a straight, Euler-Bernoulli beam for convenience of calculation. The dimensionless frequency factor is then introduced to the corresponding pipe geometry as its natural frequency deviates from the ideal beam theory. The natural frequency is given in Eq. (1) by

$$f = \lambda f_1 \tag{1}$$

with

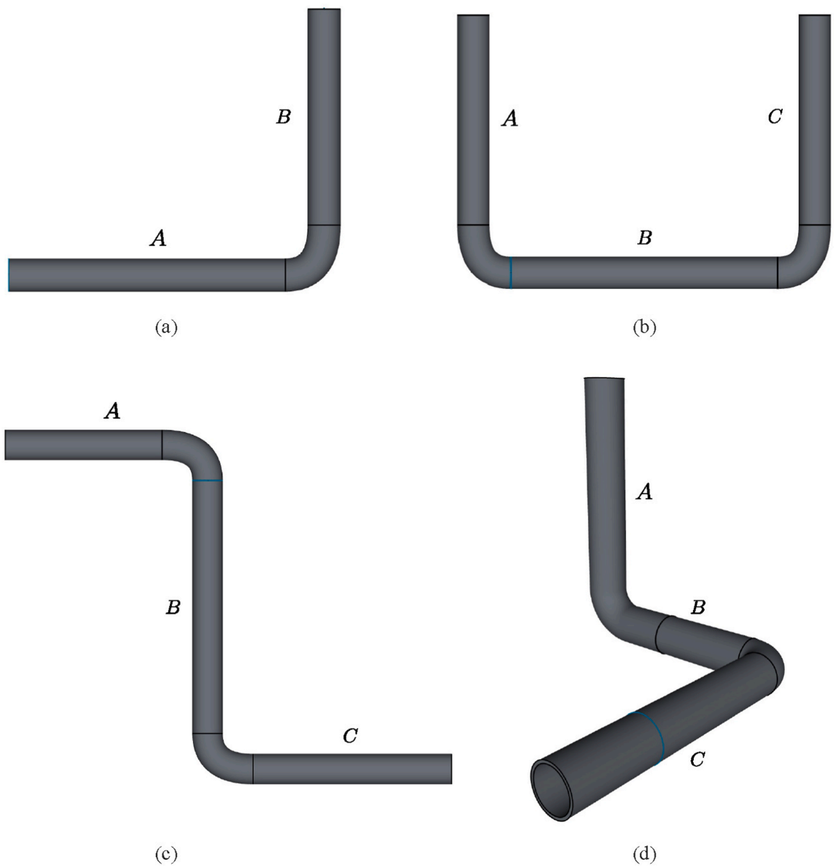

Fig. 1. Pipe geometry: (a) L-span, (b) U-span, (c) Z-span and (d) 3D-span.

Table 1
Selection of pipe diameter (OD: outside diameter, ID: inside diameter) and thickness (SCH 40).

NPS (in)	OD (mm)	Wall thickness (mm)	ID (mm)
6	168.3	7.11	154.1
12	323.9	10.31	303.3
18	457.2	14.27	428.7
24	609.6	17.48	574.6

$$f = \frac{1}{2\pi L^2}\sqrt{\frac{EI}{\mu}} \tag{2}$$

where E is the Young's modulus, L is length of pipe section, λ is frequency factor, μ is mass per unit length and I is the second mass moment of inertia given by Eq. (3)

$$I = \frac{\pi\left(D^4 - d^4\right)}{64} \tag{3}$$

with D the outer diameter and d the inner diameter of the pipe. The mass per unit area is calculated by Eq. (4)

$$\mu = \frac{1}{4}\rho\pi\left(D^2 - d^2\right) + \frac{1}{4}\rho_f \pi d^2 \tag{4}$$

where ρ is the density of the pipe and ρ_f is the density of the fluid inside the pipe. If the pipe is insulated, the mass of the insulator needs to be included to improve the accuracy of the prediction.

If the pipe has process fluid with a steady flow velocity, the natural frequency of the pipe is expressed as in Eq. (5)

$$f = \lambda f_1 C \tag{5}$$

where the correction factor to the natural frequency of the pipe is given by the following factor [2] in Eq. (6)

$$C = \sqrt{1 - \frac{\delta \rho_f \pi d^2 v^2}{4EI\beta_1^2}} \tag{6}$$

where v is the fluid velocity (m/s), $\delta = 0.55$ and $\beta_1 L = 4.730041$ for clamped edges; $\delta = 1$ and $\beta_1 L = \pi$ for simply supported edges.

2.2. Finite element analysis and λGraph

The frequency factor, λ in Eq. (1) is the important parameter highlighted in this paper. The natural frequencies of the first two modes for each pipe geometry are first simulated using Finite Element Method in ANSYS. Once the natural frequency is obtained from the simulation, the frequency factor is calculated by

$$\lambda = \frac{f_A}{f_B} \tag{7}$$

where f_A is the natural frequency obtained from ANSYS simulation. This frequency factor is calculated for various length ratios (B/A and C/A) for each pipe geometry and averaged over several pipe diameters as in Table 1 to ensure its validity over various range of pipe dimensions.

This pipe dimension requirements are referred to American Society of Mechanical Engineers (ASME) regulation for various pipe dimensions allowed for their usage in the oil and gas industry [17]. NPS stands for Nominal Pipe Size (in inch), which refers to the two times the radius of the pipe from the centre to the centreline of the pipe thickness. SCH stands for Schedule, which refers to the pipe thickness. In this analysis, SCH 40 is chosen because it is commonly used in oil and gas piping systems due to its suitability for use in heat and pressure resistant. Majority of pipelines worldwide are constructed from carbon steel [18].

In ANSYS, the length of the pipe was set to 6 m, made of carbon steel (density of $\rho = 7850$ kg/m^3) with four piping diameters as in Table 1. The length ratios of the pipe section as in Fig. 1 were $C/A = 0.25$, 0.5, 0.75 and 1, and $B/A = 0.2$, 0.4, 0.6, 0.8, 1, 2, 3, 6, 10. The mesh type was quadrilateral/hexahedral with size of 0.01 m. The convergence test (mesh sensitivity) has been done to ensure that this mesh size is sufficient to simulate accurately the first two mode shapes of the pipe.

The edges of the pipe in ANSYS are set as simply supported edges (pinned-pinned). This differs from the clamped edges assumed in Watchel et al. [16]. The simply supported edges are proposed to give less constraint motion to the pipe as not all pipes in practice are rigidly clamped (infinitely stiff), and thus pipe can have lower natural frequency. For example, the pipe which uses U-bolt clamp and hung through a rigid wall/ceiling will have more flexibility to move in horizontal direction. The flow chart to calculate the frequency factor, λ is given in Fig. 2.

2.3. Validation of the finite element (FE) model

The validation of the FE model is demonstrated by calculating the frequency factors as presented in Ref. [16] and the results of the λ-charts for the clamped edges are plotted. However, the diameters of pipe used for calculating the frequency factor, λ is not mentioned in Ref. [16]. In this paper, simulation of the FEM uses the piping diameters as listed in Table 1 and other parameters mentioned in Section 2.2. Thus, apart from validating the FE model, this also indicates that λ to predict the natural frequency of a pipe can be used for any piping diameter, material and pipe length.

Table 2 and Table 3 present the example results for the clamped-free pipe and the L-shape pipe with acceptable accuracy. The boundary condition in the FE model was then modified from the clamped edges to simply supported edges.

3. Charts of frequency factors

In this section, the frequency factor, λ-charts are plotted for clamped edges (as in Watchel et al. [16]) with additional curves for the simply supported edges. The area between the curves from the clamped edges (upper curve) and simply supported edges (bottom curve) indicates the possible range of values of the frequency factor, λ. The frequency factors for the simply supported edges has lower values than those of the clamped edges as the former has more flexibility (with rotation is less constraint at the pinned edge) allowing the pipe to have lower natural frequency.

Here, only the lowest mode shapes are considered (out-of-plane and in-plane, in a 2D-plane) and the first and second mode shapes for the 3D-span pipe, as these are the mode shapes having high vibration amplitude and mostly can be solved by constraining the pipe motion with piping supports. At higher frequency where bending vibration in pipe structure is dominant, the analysis must involve strain and stress analysis to determine possible fatigue crack in the pipe, particularly at the small-bore connection [19].

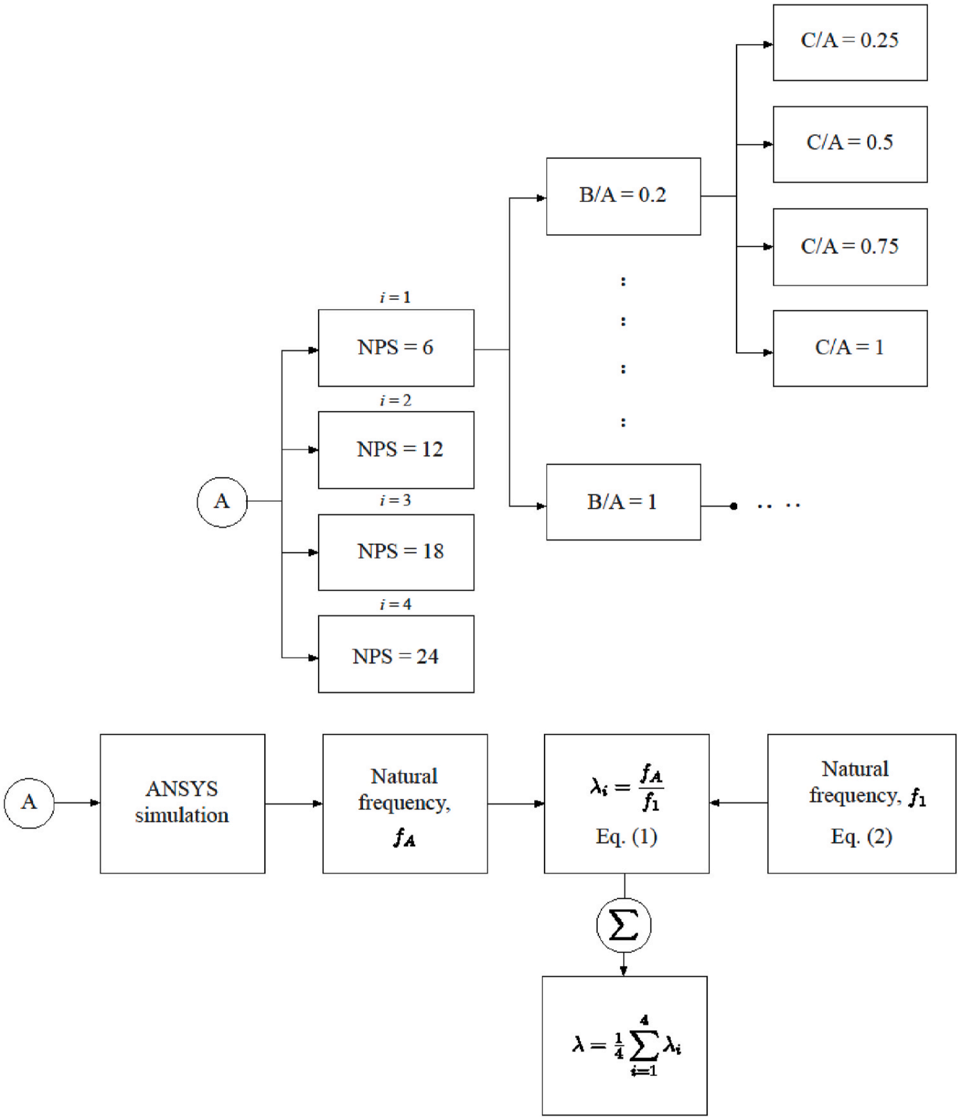

Fig. 2. The flow chart of obtaining the frequency factor.

Table 2
Calculated frequency factors for a clamped-free pipe (1st mode): carbon steel, $L = 6$ m.

Pipe dimensions (SCH- 40)	Frequency factor, λ	Averaged λ	λ from Ref. [16]	% Error
NPS-6	3.22	3.41	3.52	3.2%
NPS-12	3.39			
NPS-18	3.69			
NPS-24	3.32			

Table 3
Calculated frequency factors for a clamped-clamped L-shape pipe (out-of-plane mode): carbon steel, $B/A = 0.4$, $L = 6$ m.

Pipe dimensions (SCH- 40)	Frequency factor, λ	Averaged λ	λ from Ref. [16]	% Error
NPS-6	21.3	22.1	22.5	1.8%
NPS-12	24.2			
NPS-18	22.3			
NPS-24	20.3			

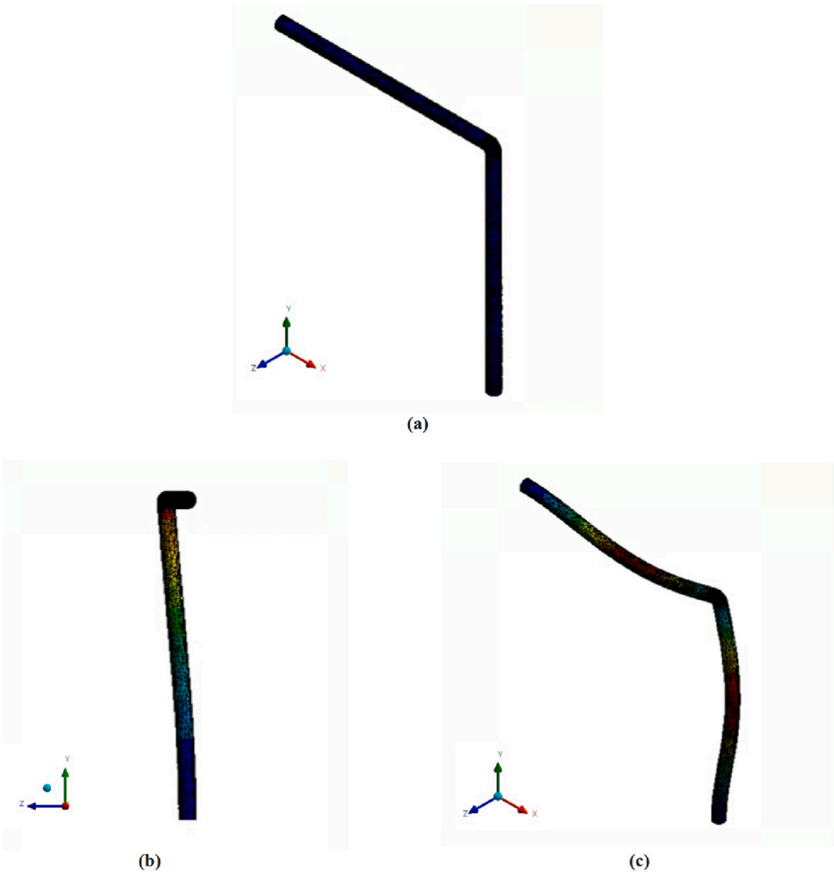

Fig. 3. Mode shapes of the L-span pipe from ANSYS: (a) 3D view, (b) out-plane mode and (c) in-plane.

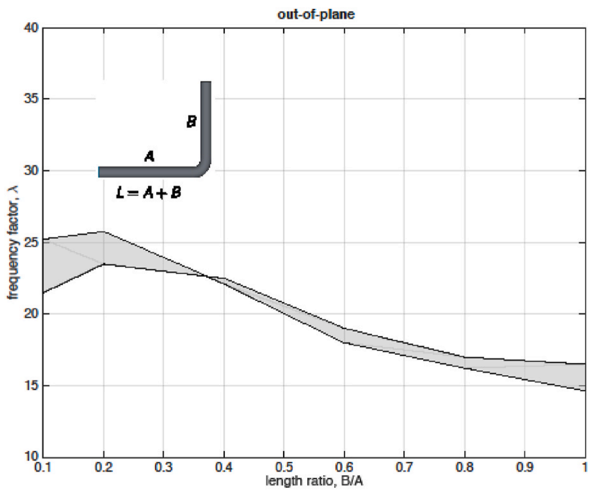

Fig. 4. Graph of frequency factor for L-span pipe: out-of-plane 1st mode.

3.1. L-span pipe

Fig. 3 shows the mode shape of the L-span pipe simulated from ANSYS. The out-of-plane mode (in Fig. 3(b)) has low frequency as the pipe is more flexible in horizontal direction (z-axis). In practice, this type of mode is the most common due to turbulence-induced excitation which is usually at low frequency range. The in-plane mode (in Fig. 3(c)) is more difficult to be generated as the pipe is stiffer

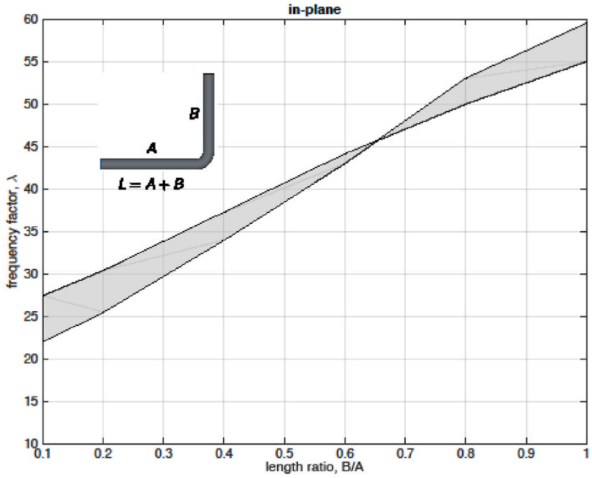

Fig. 5. Graph of frequency factor for L-span pipe: in-plane 1st mode.

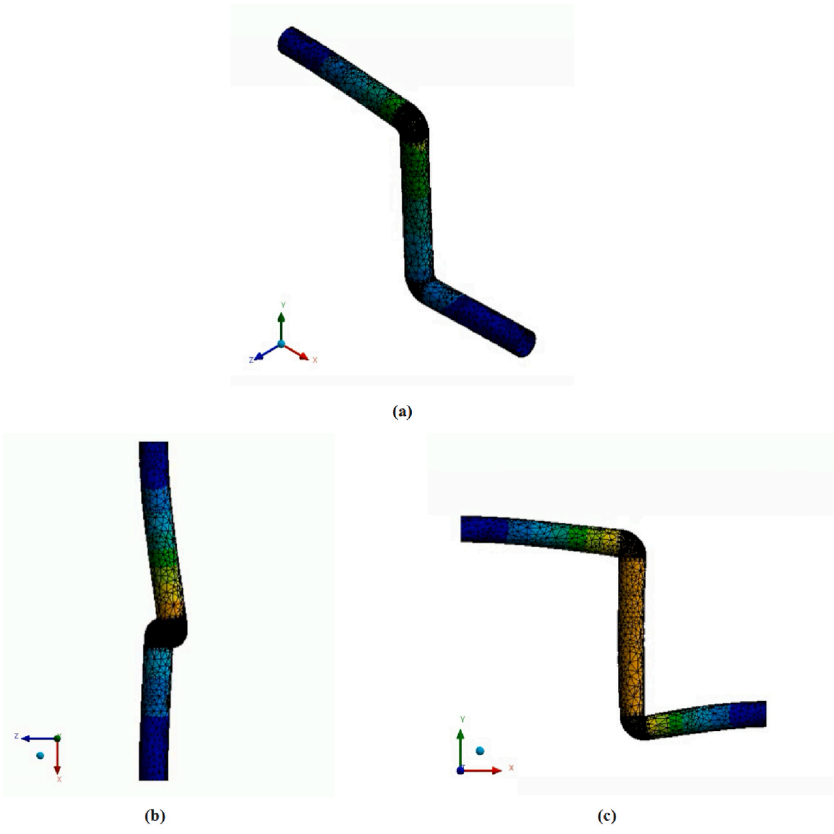

Fig. 6. Mode shapes of the Z-span pipe from ANSYS: (a) 3D view, (b) out-of-plane mode and (c) in-plane mode.

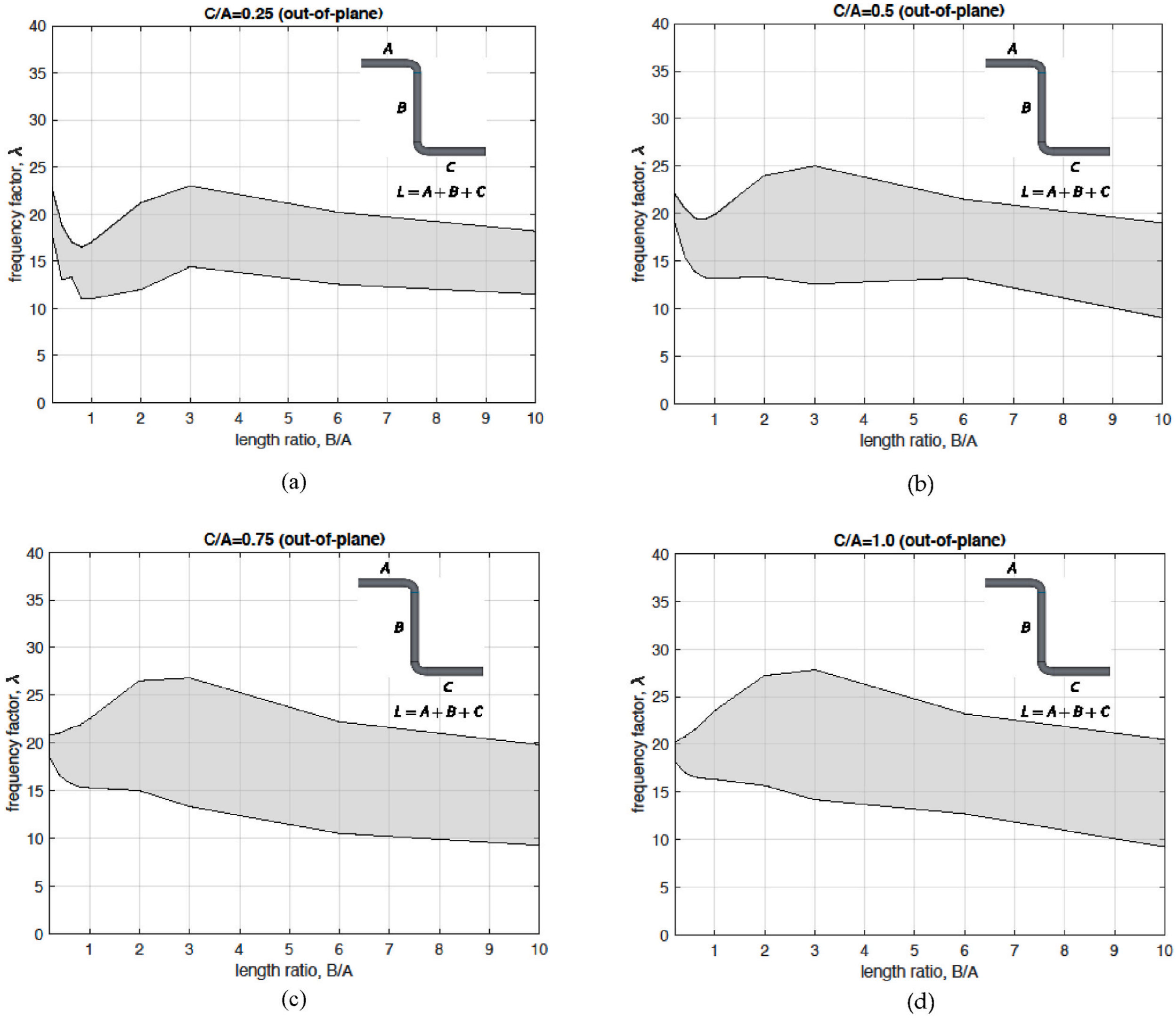

Fig. 7. Graph of frequency factor for Z-span pipe out-of-plane 1st mode. (a) $C/A = 0.25$, (b) $C/A = 0.5$, (c) $C/A = 0.75$ and $C/A = 1.0$.

in the longitudinal direction (*xy*-plane). High vibration force from water hammer can possibly excite this mode.

The frequency factor graphs as the function of pipe length ratio for the first mode of out-of-plane and in-plane modes are shown in Figs. 4 and 5.

3.2. Z-span pipe

Fig. 6 shows the mode shape of the Z-span pipe. Similar to the L-span, the out-plane mode (in Fig. 6(b)) is more flexible in horizontal direction (*z*-axis) compared to the in-plane mode (*xy*-plane) (in Fig. 6(c)).

Figs. 7 and 8 present the frequency factor graphs for the out-plane and in-plane modes of the Z-span pipe, respectively. For clarity, the graphs are separated in terms of the length ratio, C/A.

The high peak in Fig. 8 for the in-plane mode reveals that for $C/A = 0.25$ (in Fig. 8(a)), the length of A and B is so small making it too stiff for the in-plane mode to be generated along the xy-plane. This is however applied for the clamped edges. As the edges are less constraint (simply supported), the frequency factor can be seen to be significantly reduced.

3.3. U-span pipe

Fig. 9 shows the mode shape of the U-span pipe. The frequency factor graphs as the function of length ratio are shown in Figs. 10 and 11. As for the Z-span pipe, the in-plane mode for $C/A = 0.25$ (in Fig. 11(a)) show high peak at $B/A = 1$ and significantly reduce above $B/A = 1.0$.

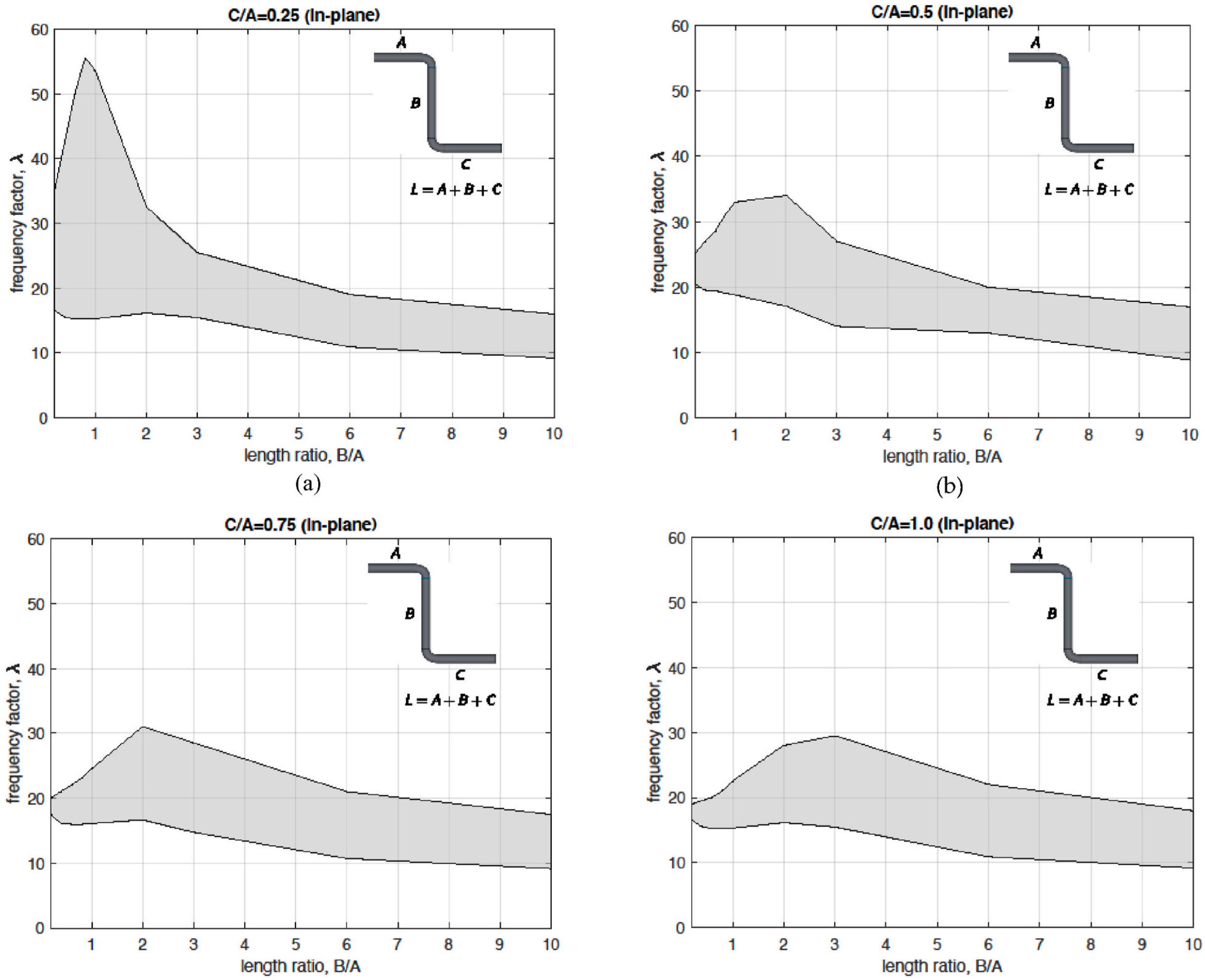

(a) (b) (c) (d)

Fig. 8. Graph of frequency factor for L-span pipe in-plane 1st mode. (a) $C/A = 0.25$, (b) $C/A = 0.5$, (c) $C/A = 0.75$ and $C/A = 1.0$.

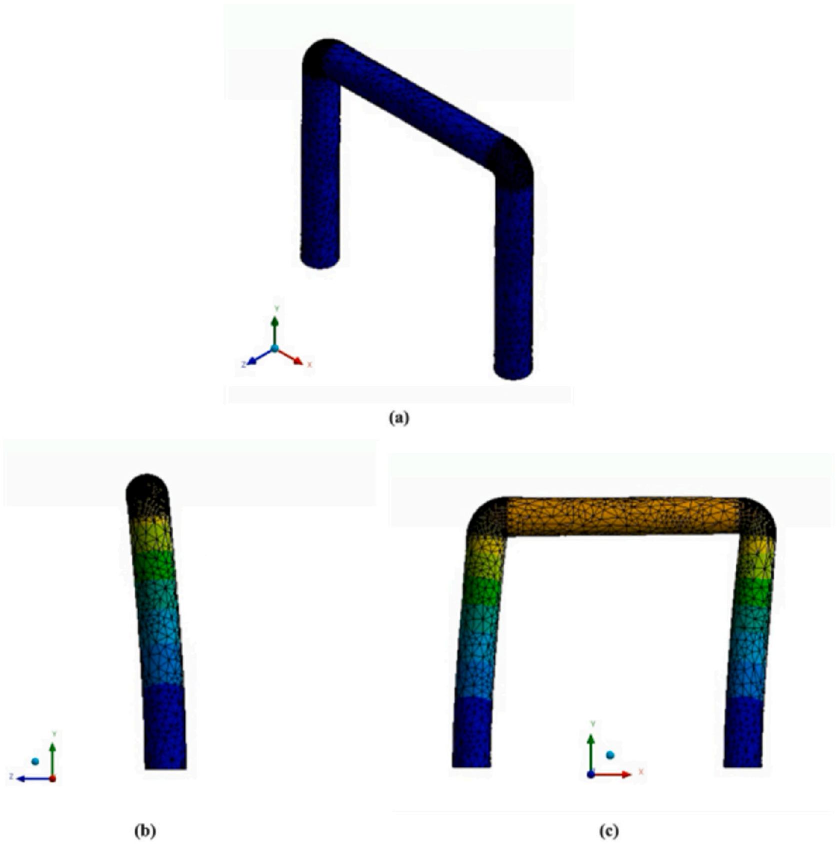

Fig. 9. Mode shapes of the U-span pipe from ANSYS: (a) 3D view, (b) out-plane mode and (c) in-plane mode.

3.4. 3D-span pipe

The mode shapes for the 3D span pipe from ANSYS is shown in Fig. 12. The 1st mode (in Fig. 12(b)) is when the vertical section of the pipe and the horizontal bottom section have dominant motion in z-axis. For the 2nd mode (in Fig. 12(c)), the vertical section and the horizontal upper section have dominant motion in x-axis.

Figs. 13 and 14 are the frequency factor graphs for the 1st mode and 2nd mode, respectively. Again, the high peak in the 2nd mode for $C/A = 0.25$ (in Fig. 14(a)) is because the length of the horizontal upper section is too small, so that the stiffness along x-axis is high (see again Fig. 12(c)).

4. Experimental verification

Fig. 15 shows diagram of a pipe to supply oxygen (density 1.43 g/L) into a burner and had been found to excessively vibrate at 63 Hz in horizontal direction (x-axis). A bump test was thus conducted to estimate the natural frequency of the pipe. This was a vibration analysis project conducted in one of a refinery process industry in Malaysia. The test was performed during a planned shutdown where the refinery process was offline. The pipe was bumped using an instrumented hammer (Dytran) and an accelerometer sensor (ICP Wilcoxon) was attached along the ABCD line to measure the signal during the strike. The data was processed in a portable analyzer (VABBIT PRO, 4-channel DAQ system). Section DE was connected to a larger pipe diameter, and thus its motion in x-direction is mostly restricted. The measurement at DE section revealed that the vibration level was significantly lower compared to the vibration at ABCD line.

The result is shown in Fig. 16, showing that the first natural frequency is around 73.5 Hz. This is the measured result when the pipe was hit in horizontal direction (x-axis, out-of-plane mode). In this study case, the piping vibration of 63 Hz was within the resonance as it is in the range ±25% of its natural frequency. For predicting the natural frequency, only ABCD section of the pipe is considered as along this location was where the pipe had significant vibration level. Therefore, for the analysis, the piping here is assumed to have Z-span.

The edge at point A is connected to a burner and can be assumed to have a clamped edge, but at point D the edge has certain degree of flexibility. The pipe is made of carbon steel (density 7850 kg/m^3), and has outer diameter of 6-in and thickness of 4 mm. By using Eqs. (1)–(4) and using the chart in Fig. 7 for $C/A = 0.75$ and for $B/A = 1.5$, the predictive range of the natural frequency is 58 Hz (if

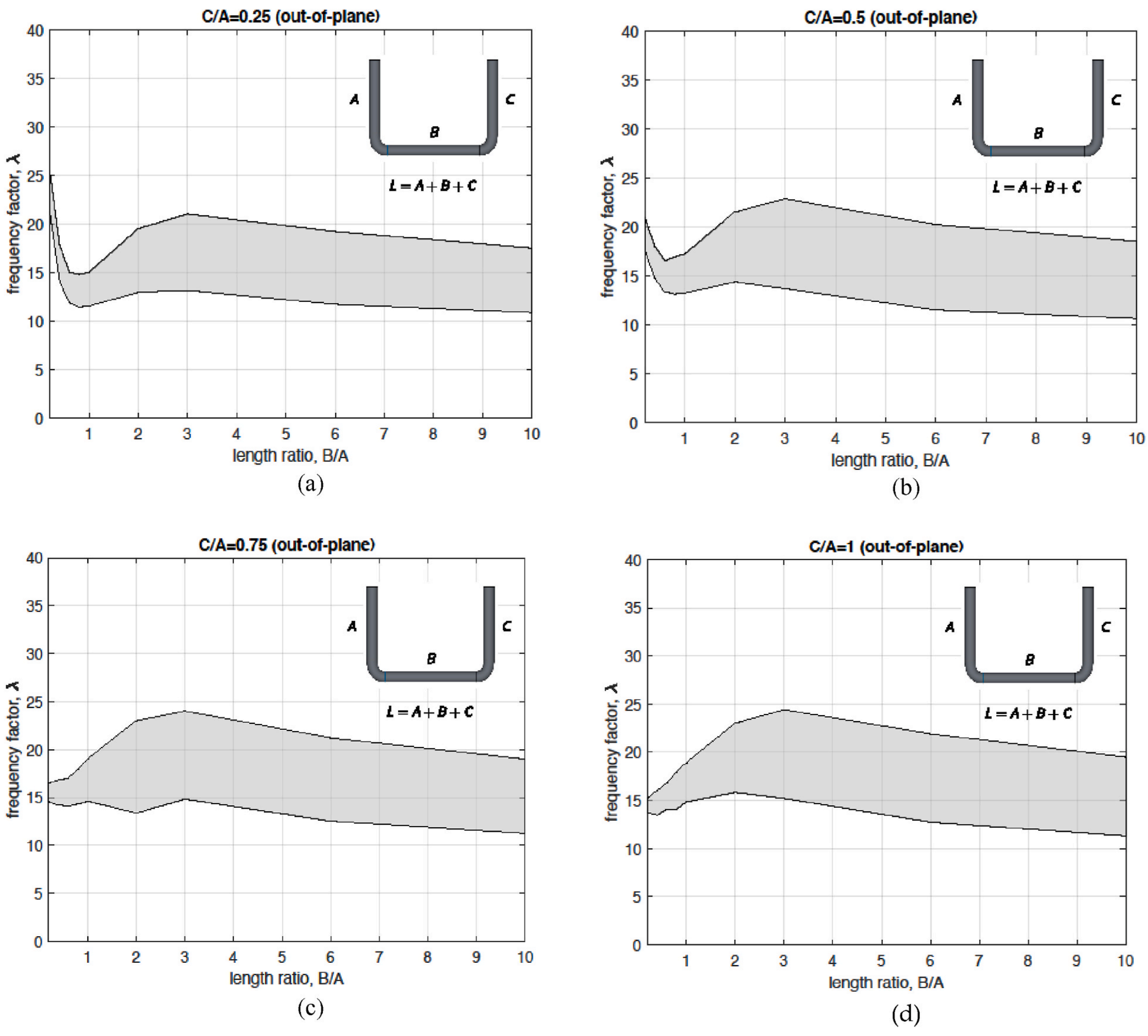

Fig. 10. Graph of frequency factor for U-span pipe out-plane 1st mode. (a) $C/A = 0.25$, (b) $C/A = 0.5$, (c) $C/A = 0.75$ and $C/A = 1.0$.

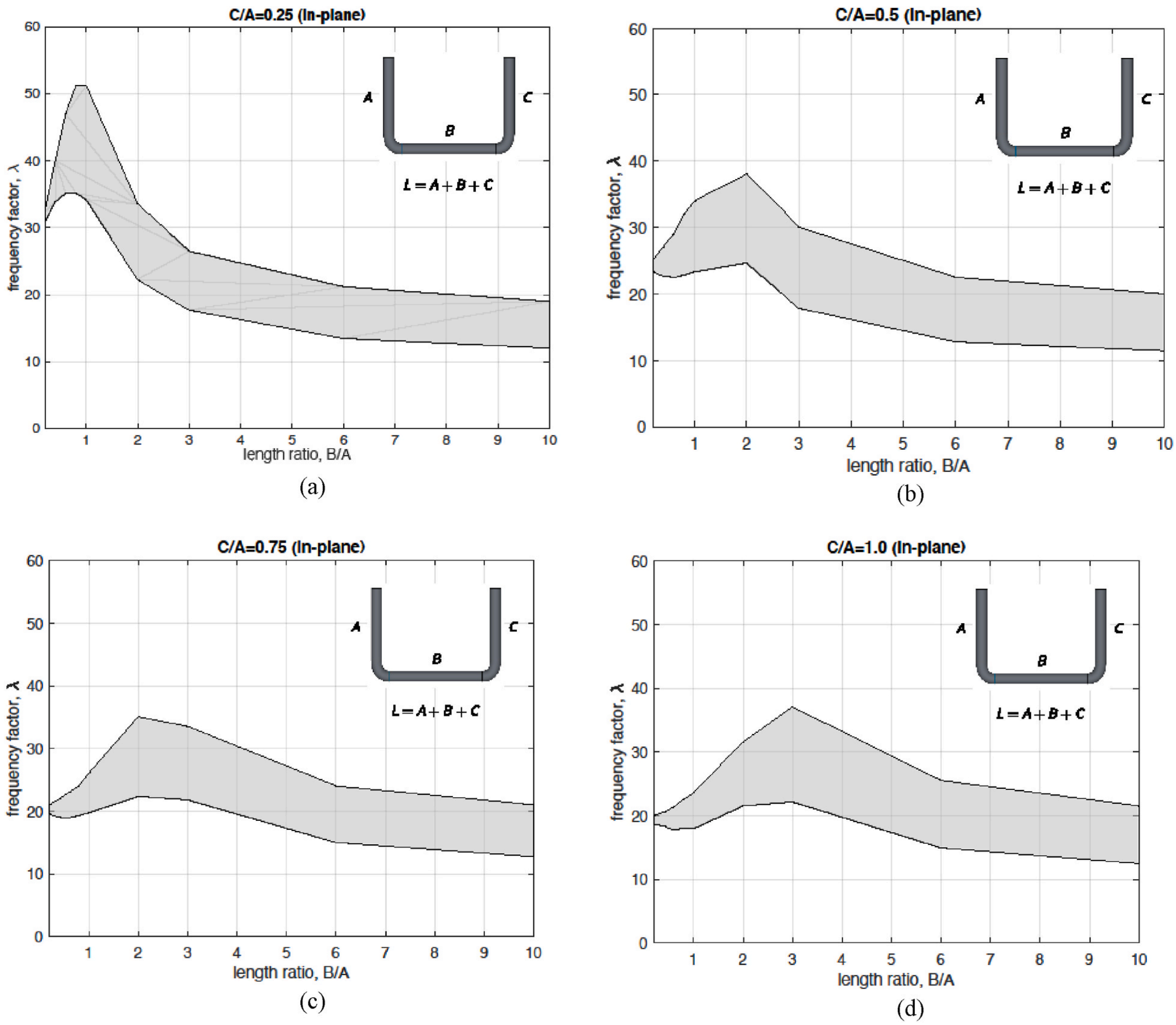

Fig. 11. Graph of frequency factor for U-span pipe in-plane 1st mode. (a) $C/A = 0.25$, (b) $C/A = 0.5$, (c) $C/A = 0.75$ and $C/A = 1.0$.

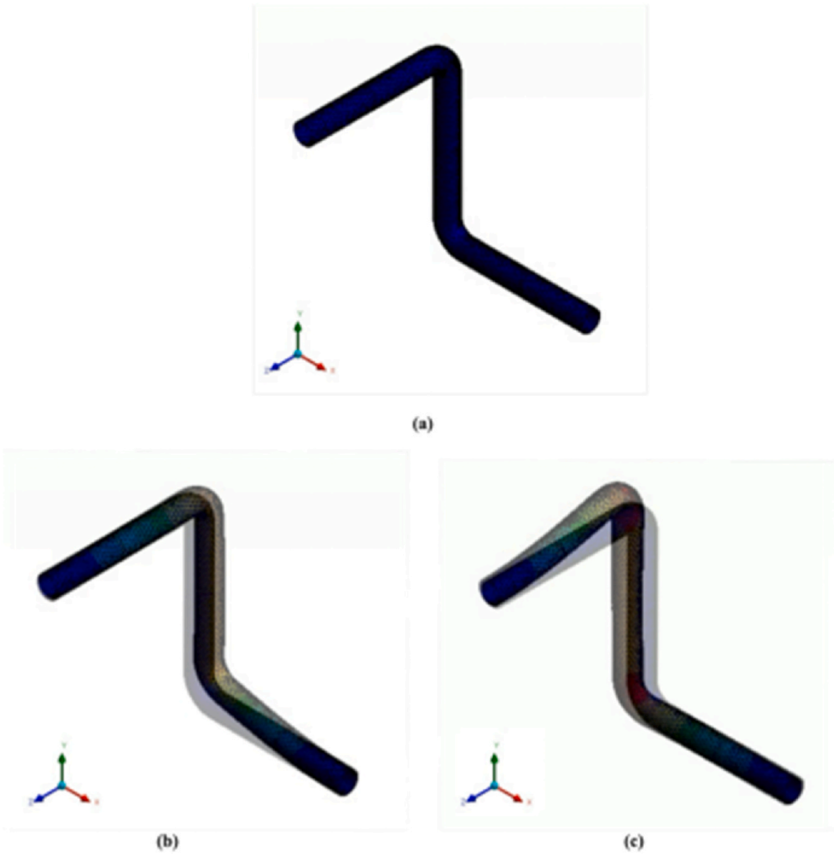

Fig. 12. Mode shapes of the 3D-span pipe from ANSYS: (a) 3D view, (b) 1st mode and (c) 2nd mode.

both edges are simply supported) to 93 Hz (if both edges are fully clamped). The measured natural frequency is 73.5 Hz, which is between these two values. The chart thus serves its purpose to provide a quick prediction of piping natural frequency for engineers on site to judge whether the piping vibration can be considered a resonance before a proper test is performed to measure the natural frequency.

5. Conclusion

Correction factor charts of piping natural frequencies for various piping configurations has been proposed for clamped and simply supported edges. The natural frequencies of the pipe were calculated using ANSYS, and the prediction formula is based on the natural frequency of a Euler-Bernouli beam. To compensate the various pipe configurations, correction factors are produced. By considering these two edges, the frequency factors can be presented in the range of possible values. These charts are aimed at providing engineers to have a convenient prediction of corresponding pipe natural frequency when a problem from piping vibration arises, so that a correct troubleshooting action can be performed before a thorough vibration analysis is conducted. However, the proposed charts are only for the 1st mode of vibration. The future work can be extended into the 2nd mode of vibration especially for the pipe spans in 2D-plane (L, Z, and U shapes). Laboratory experiment with various types of piping supports is also of interest to validate the robustness of the proposed charts.

Data availability

Available from the first author upon request.

Funding statement

This research received no external funding.

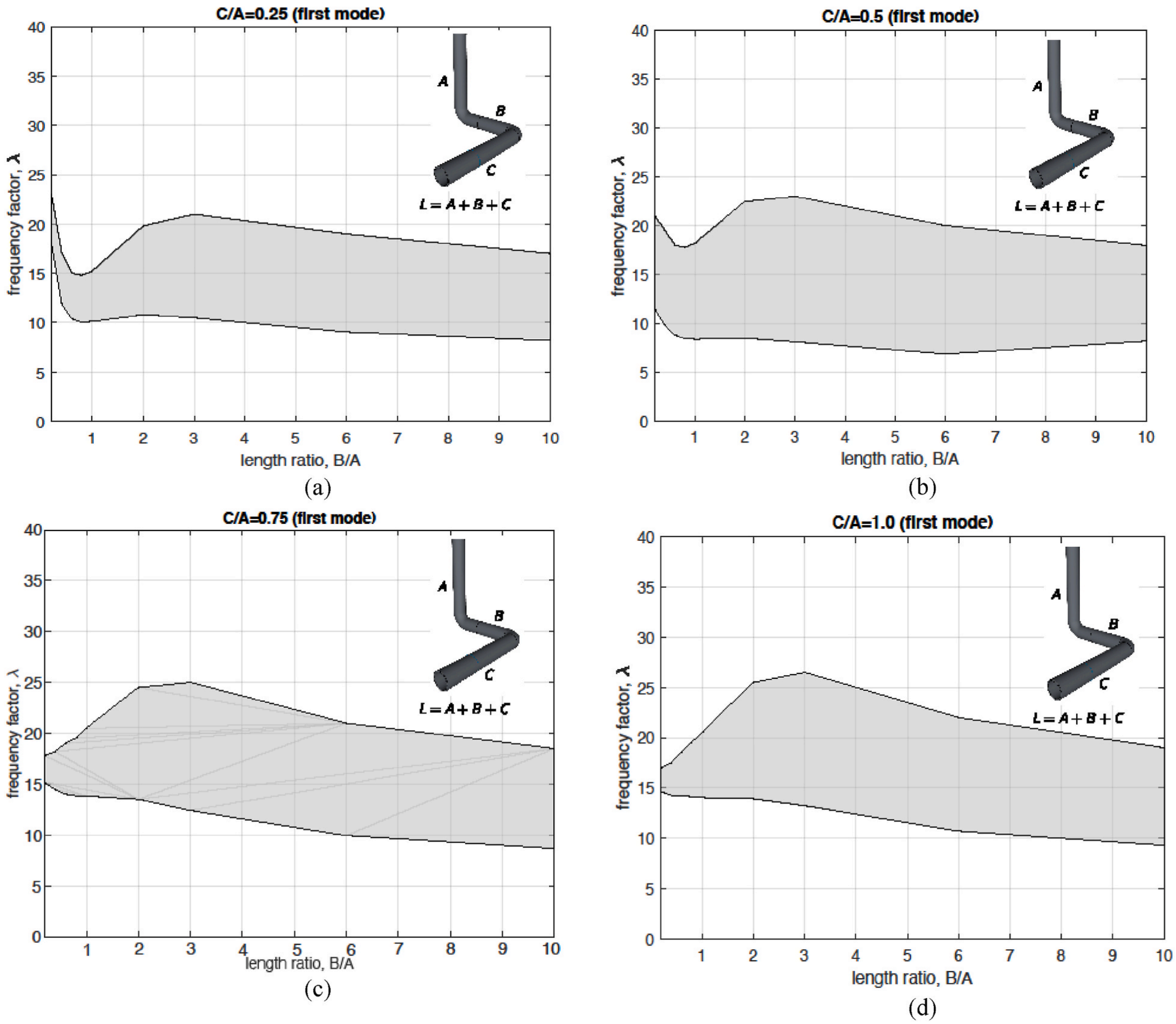

Fig. 13. Graph of frequency factor for 3D-span pipe: 1st mode. (a) $C/A = 0.25$, (b) $C/A = 0.5$, (c) $C/A = 0.75$, and $C/A = 1.0$.

Additional information

No additional information is available for this paper.

CRediT authorship contribution statement

Noor Fariza Saari: Writing – review & editing, Writing – original draft, Visualization, Validation, Software, Methodology, Investigation. **Azma Putra:** Writing – review & editing, Writing – original draft, Validation, Methodology, Formal analysis, Conceptualization. **Irianto:** Harny, Resources, Project administration, Funding acquisition, Data curation. **Reduan Mat Dan:** Validation, Methodology. **Muhammad Agus Zeli:** Writing – original draft, Visualization, Software, Methodology, Investigation. **Roszaidi Ramlan:** Validation, Methodology, Investigation, Formal analysis, Data curation. **Nawal Aswan Abdul Jalil:** Writing – original draft, Methodology, Investigation, Formal analysis. **Safarudin Herawan:** Project administration, Funding acquisition, Data curation.

Declaration of competing interest

The authors declare that they have no known competing financial interests or personal relationships that could have appeared to influence the work reported in this paper.

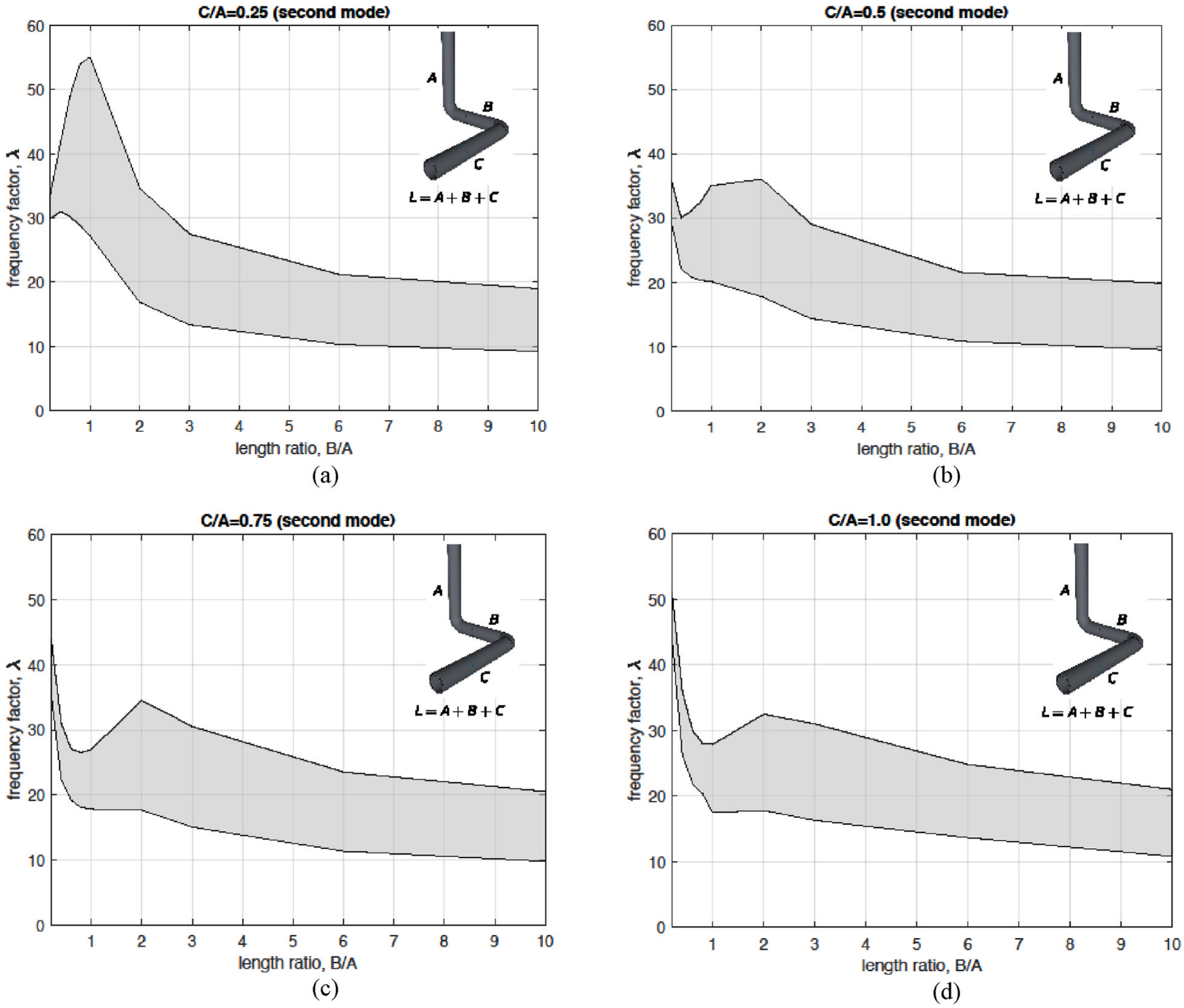

Fig. 14. Graph of frequency factor for 3D-span pipe: 2nd mode. (a) $C/A = 0.25$, (b) $C/A = 0.5$, (c) $C/A = 0.75$ and $C/A = 1.0$.

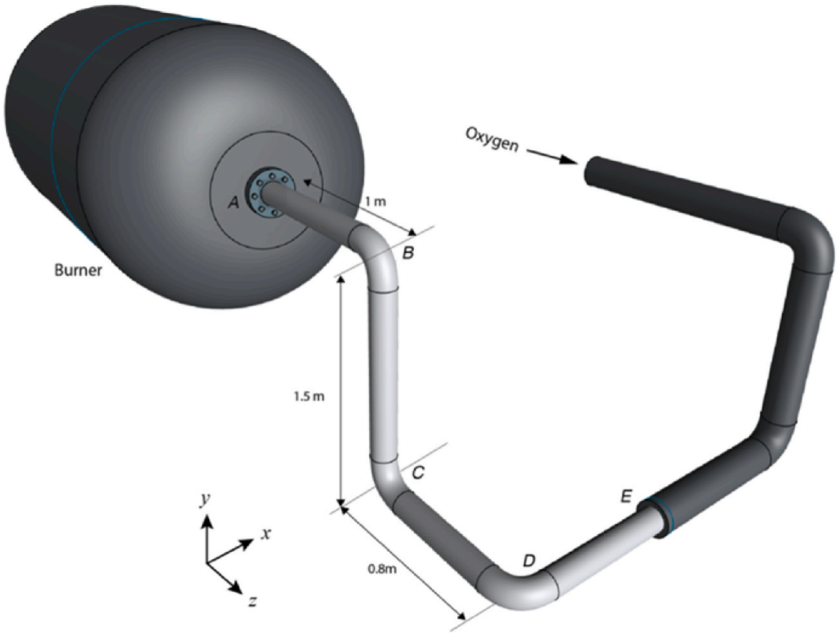

Fig. 15. Diagram of a steel pipe supplying oxygen to a burner unit.

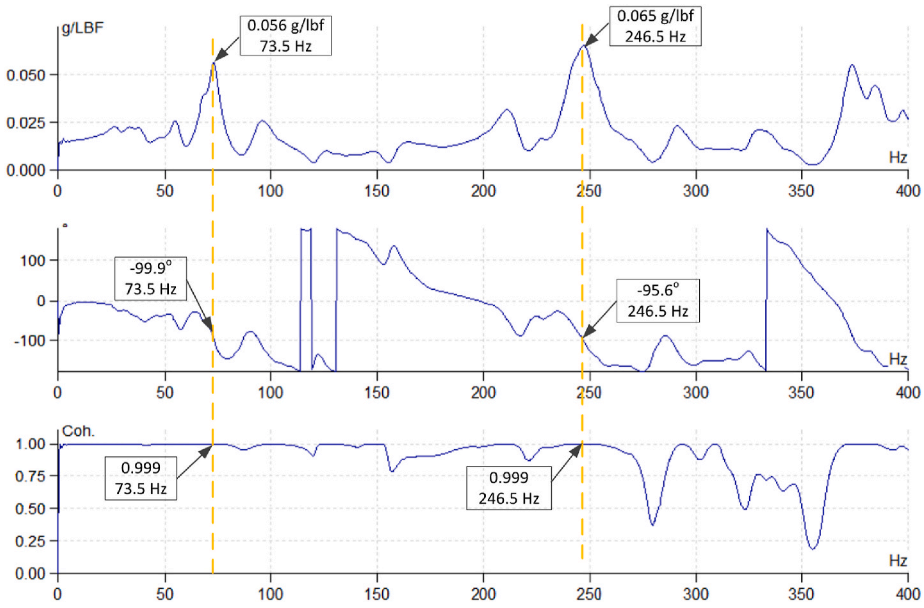

Fig. 16. Measured spectrum from bump test in x-axis: amplitude (top), phase (middle) and coherence (bottom).

References

[1] N. Sukaih, A practical, systematic and structured approach to piping vibration assessment, Int. J. Pres. Ves. Pip. 79 (2002) 597–609.

[2] H. Yi-Min, L. Yong-Shou, L. Bao-Hui, et al., Natural frequency analysis of fluid conveying pipeline with different boundary conditions, Nucl. Eng. Des. 240 (3) (2010) 461–467.

[3] G. Liu, Y. Wang, Natural frequency analysis of a cantilevered piping system conveying gas–liquid two-phase slug flow, Chem. Eng. Res. Des. 136 (2018) 564–580.

[4] Yi-min Huang, Senga Ge, Weia Wu, Jieb He, A direct method of natural frequency analysis on pipeline conveying fluid with both ends supported, Nucl. Eng. Des. 253 (2012) 12–22.

[5] Bao-hui Li, Hang-shan Gao, Hong-bo Zhai, Yong-shou Liu, Zhu-feng Yue, Free vibration analysis of multi-span pipe conveying fluid with dynamic stiffness method, Nucl. Eng. Des. 241 (3) (2011) 666–671.

[6] Tijsseling, S. Arris, Alan E. Vardy, D. Fan, Fluid-structure interaction and cavitation in a single-elbow pipe system, J. Fluid Struct. 10 (4) (1996) 395–420.

[7] Yu-Jia Hua, Weidong Zhub, Vibration analysis of a fluid-conveying curved pipe with an arbitrary undeformed configuration, Appl. Math. Model. 64 (2018) 624–642.
[8] Jijun Gu, Tianqi Ma, Menglan Duan, Effect of aspect ratio on the dynamic response of a fluid-conveying pipe using the Timoshenko beam model, Ocean. Eng. 114 (2016) 185–191.
[9] G.H. Koo, Y.S. Park, Vibration analysis of a 3-dimensional piping system conveying fluid by wave approach, Int. J. Pres. Ves. Pip. 67 (3) (1996) 249–256.
[10] Lin Zhang, Tao Zhang, Huajiang Ouyang, Tianyun Li, Mo You, Natural frequency assignment of a pipeline through structural modification in layout optimization of elastic supports, J. Sound Vib. 561 (2023) 117702.
[11] R. Veerapandi, G. Karthikeyan, G.R. Jinu, R. Kannaiah, Experimental study and analysis of flow induced vibration in a pipeline, Int. J. Eng. Res. Technol. 3 (5) (2014).
[12] Kaiming Bi, Hong Hao, Using pipe-in-pipe systems for subsea pipeline vibration control, Eng. Struct. 109 (2016) 75–84.
[13] Mehrdad Shemshadi, Mahdi Karimi, Farzad Veysi, A simple method to design and analyze dynamic vibration absorber of pipeline structure using dimensional analysis, Shock Vib. 2020 (2020) 1–13. Article ID 2478371.
[14] Mouloud Dahmane, Djilali Boutchicha, Lahouari Adjlout, One-way fluid structure interaction of pipe under flow with different boundary conditions, Mechanics 22 (2016) 495–503.
[15] J. Medeiros, C.O. Mendonca, E.B. Tinoco, Dynamic analysis of a reciprocating compressor piping system, in: Proceedings of Rio Oil & Gas Expo Conference, Rio De Janeiro, 2020.
[16] J.C. Wachel, S.J. Morton, K.E. Atkins, Piping vibration analysis, in: Proceedings of the 19th Turbomachinery Symposium, Texas A&M University, Turbomachinery Laboratories, 1990, 1990.
[17] ASME B36.10M, Welded and Seamless Wrought Steel Pipe, The American Society of Mechanical Engineers, 2018.
[18] K. Sotoodeh, Chapter 13-Piping and valve corrosion study, in: K. Sotoodeh (Ed.), A Practical Guide to Piping and Valves for the Oil and Gas Industry, Gulf Professional Publishing, 2021, pp. 585–627, 2021.
[19] Energy Institute, Guidelines for the Avoidance of Vibration Induced Fatigue in Process Pipeworks, second ed., 2008. London.